Supporting Information

Glucose Oxidase-Catalyzed Growth of Gold Nanoparticles Enables Quantitative Detection of Attomolar Cancer Biomarkers

Dingbin Liu,[†] Jie Yang,[†] He-Fang Wang,[†] Zhongliang Wang,*[‡] Xinglu Huang,[‡] Zhantong Wang,[§] Gang Niu,[‡] A. R. Hight Walker,[¶] and Xiaoyuan Chen*[‡]

[†] State Key Laboratory of Medicinal Chemical Biology, Collaborative Innovation Center of Chemical Science and Engineering, and Research Center for Analytical Sciences, College of Chemistry, Nankai University, Tianjin (China)

[‡]Laboratory of Molecular Imaging and Nanomedicine (LOMIN), National Institute of Biomedical Imaging and Bioengineering (NIBIB), National Institutes of Health (NIH), Bethesda, Maryland 20892 (USA)

[§] State Key Laboratory of Molecular Vaccinology and Molecular Diagnostics & Center for Molecular Imaging and Translational Medicine, School of Public Health, Xiamen University, Xiamen 361005 (China)

[¶]Optical Technology Division, Physics Laboratory, National Institute of Standards and Technology, Gaithersburg, Maryland 20899 (USA)

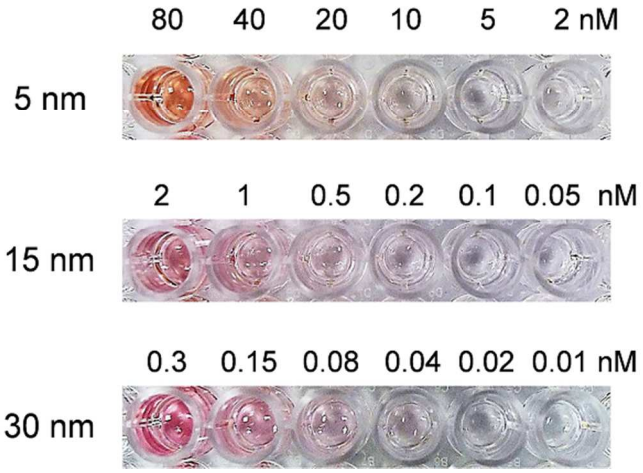

Figure S1. Color of various concentrations of AuNP solutions with different sizes of the particles.

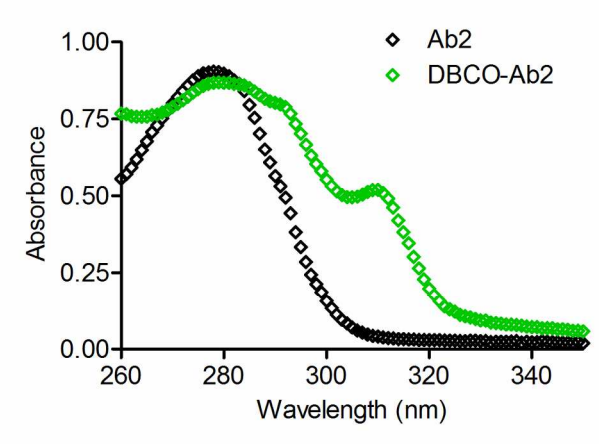

Figure S2. UV-vis absorption spectra of purified PSA detection antibody (black) and that labeled with dibenzocyclooctyl (DBCO) moieties (green). The absorption band at 309 nm indicates the DBCO moieties on Ab2.

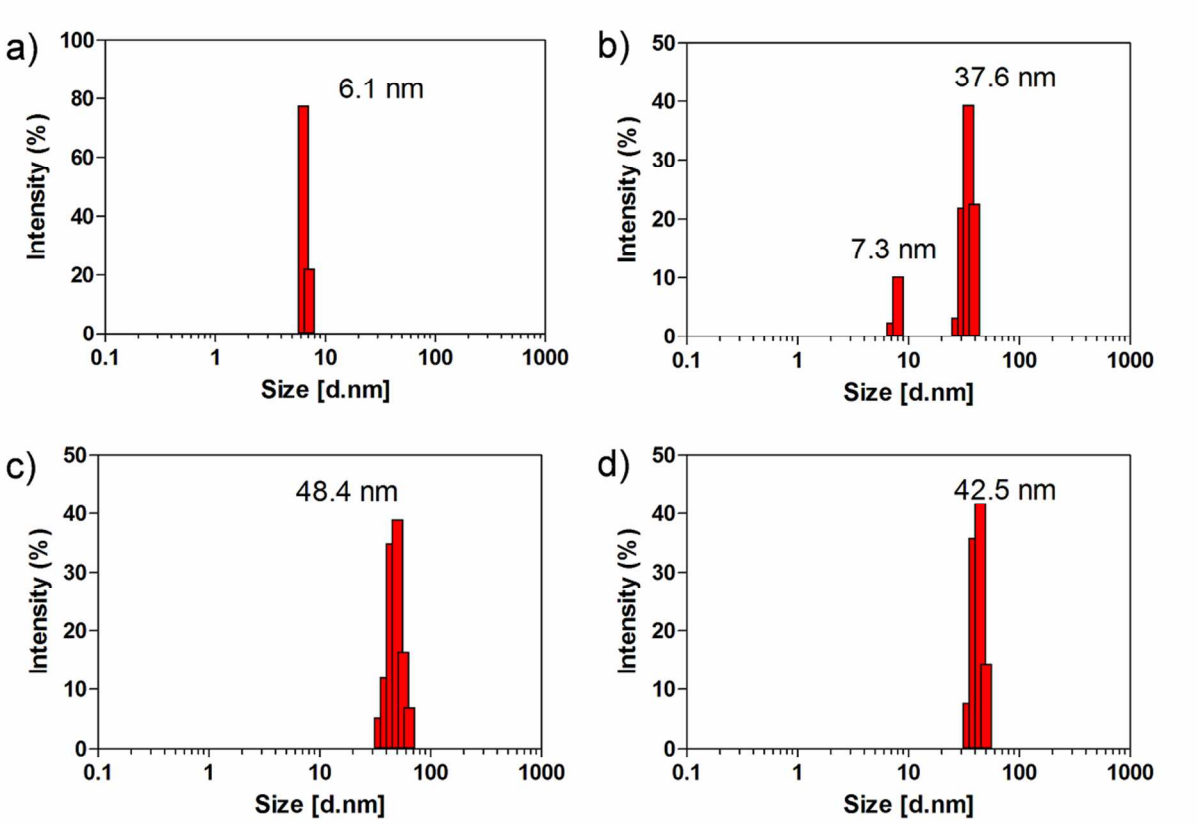

Figure S3. Dynamic light scattering (DLS) analysis of 5 nm AuNP seeds (a) and those in the presence of $HAuCl_4$ (0.6 mM) and 10 (b), 100 (c), and 1000 (d) μM of H_2O_2 respectively.

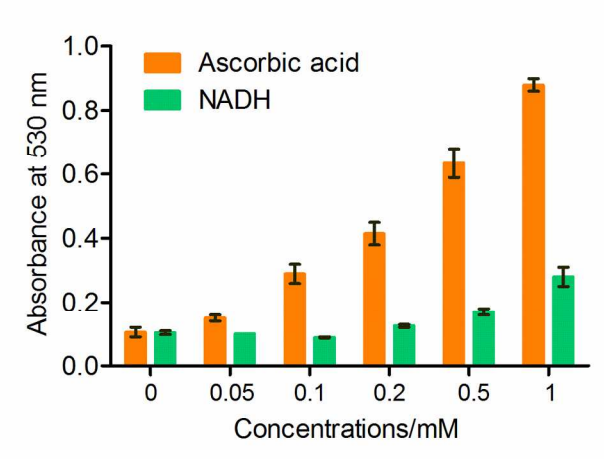

Figure S4. Various concentrations of ascorbic acid and nicotinamide adenine dinucleotide (NADH) cause the growth of 5 nm AuNPs respectively, which was indicated by the absorbance at 530 nm. Error bars show the standard deviations of three independent measurements.

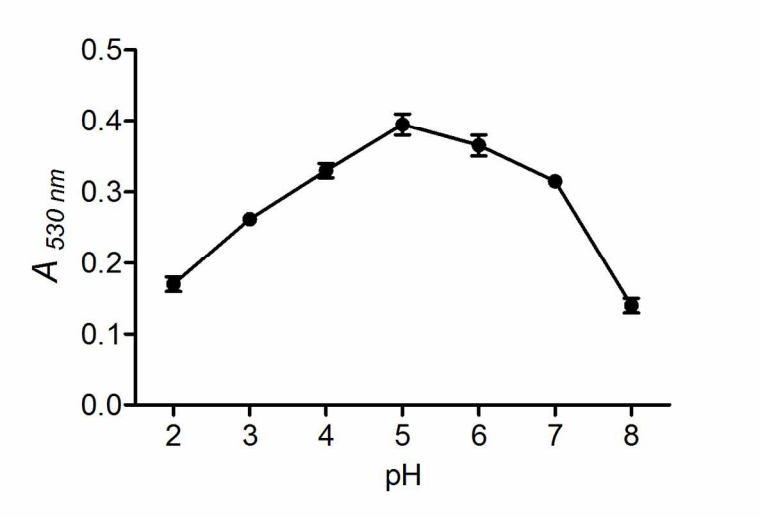

Figure S5. The effect of pH values on the biocatalytic reaction of glucose oxidase with glucose, which was monitored by the colorless-to-red assay. Error bars show the standard deviations of three independent measurements.

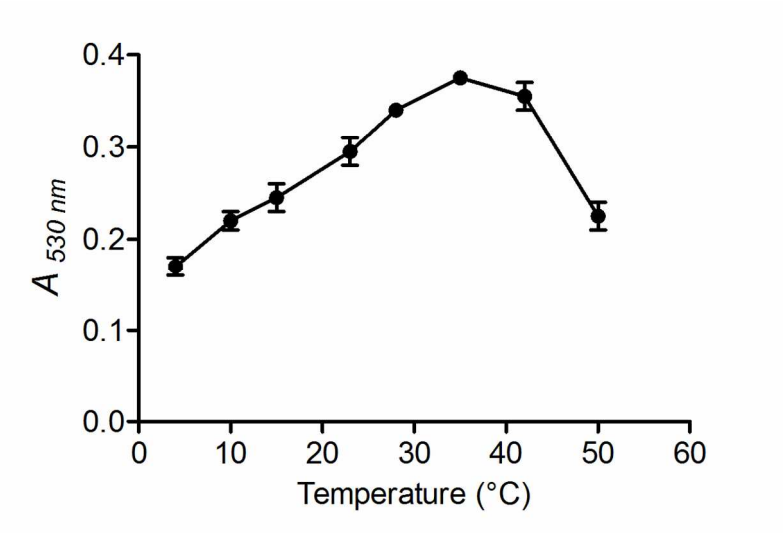

Figure S6. The effect of temperatures on the biocatalytic reaction of glucose oxidase with glucose, which was monitored by the colorless-to-red assay. Error bars show the standard deviations of three independent measurements.

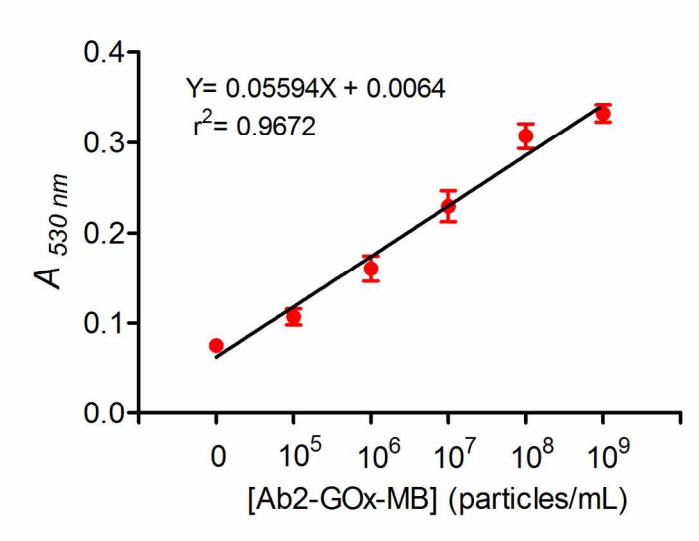

Figure S7. Detection of the colorless-to-red assay for various concentrations of Ab2-GOx-MB ranging from 10^5 to 10^9 particles/mL. Error bars show the standard deviations of three independent measurements.

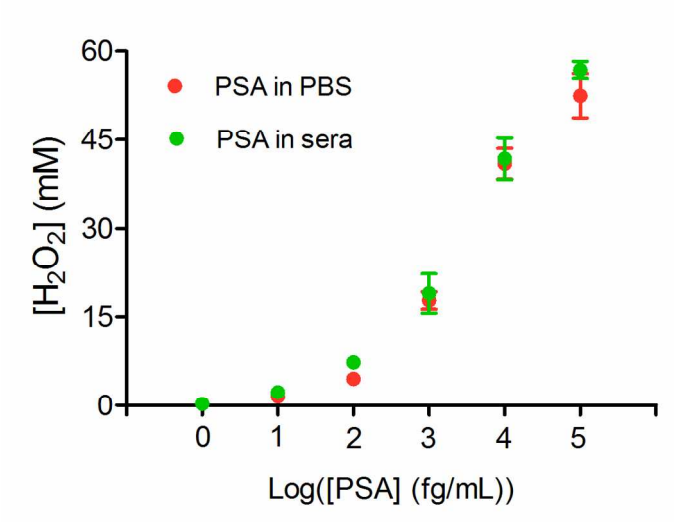

Figure S8. Measurements of the generated H_2O_2 by a H_2O_2 Assay Kit (ab102500) for various concentrations of PSA spiked in PBS and sera respectively. Error bars show the standard deviations of three independent measurements.

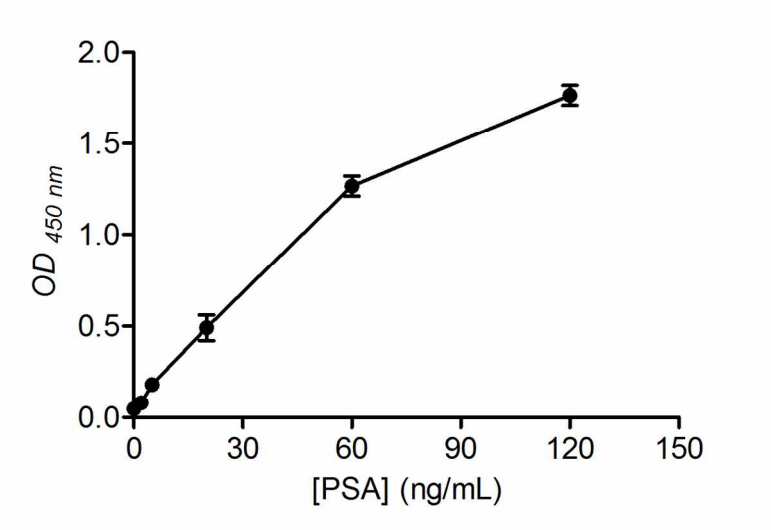

Figure S9. HRP-based ELISA for the detection of various concentrations of PSA spiked in fetal bovine sera. The OD values at 450 nm were recored by a Synergy 2 Multi-Mode Microplate Reader. Error bars show the standard deviations of three independent measurements.

Table S1 A comparison of detection performance for biosensors based on nanotechnology.

Readout	Target	Nanomater-ial	Linear range	Detection limit	Real sample	Ref.
Fluorescence	PSA	MPs	N/A	1.5 fg/mL	Serum	[1]
Fluorescence	CEA	Au film	0.2 pg/mL−20 ng/mL	1 pg/mL	Serum	[2]
Fluorescence	Troponin I	Chimeric NPs	0.1 pg/mL−10 ng/mL	0.1 fg/mL	Serum	[3]
Fluorescence	CEA	QDs	5 pg/mL−50 ng/mL	0.5 ng/mL	Serum	[4]
Electrochemistry	IL-6	SWNTs	N/A	0.5 pg/mL	Serum	[5]
Electrochemistry	IL-8	MPs	1−500 fg/mL	1 fg/mL		[6]
Electrochemistry	Thrombin	MPs	0.001–100 ng/mL	0.2 pg/mL	N/A	[7]
Electrochemistry	CEA	AuNPs	0.01–160 ng/mL	0.005 ng/mL	Serum	[8]
Scanometric	PSA	AuNPs	0.1 fg–10 pg/mL	1 fg/mL	N/A	[9]
Scanometric	HIV	AuNPs	N/A	N/A	blood	[10]

SPR	PSA	MPs	N/A	10 fg/mL	Serum	[11]
DLS	PSA	AuNPs	0.1−10 ng/mL	0.1 ng/mL	N/A	[12]
Raman	aPR3	SWNTs	N/A	0.15 pg/ml	Serum	[13]
Raman	VEGF	AuNPs	0.1−10 ng/mL	7 fg/mL	Blood	[14]
Plasmonics	PSA	AuNSs	10^{-18}–10^{-14} g/mL	10^{-18} g/mL	Serum	[15]
Plasmonics	HIV	AuNPs	N/A	98 ± 39 copies/mL	Blood	[16]
Colorimetric	PSA and P24	AuNPs	N/A	1×10^{-18} g/mL	Serum	[17]
Colorimetric	PSA	AuNPs	0.05−20 ng/mL	0.03 ng/mL	Serum	[18]
Colorimetric	EV71	AuNPs	N/A	1×10^{4} copies/mL	HTS	[19]
Colorimetric	PSA	AuNPs	10−10^{5} fg/mL	4.6 fg/mL	Serum	This study

Abbreviation: PSA, prostate-specific antigen; MPs, magnetic particles; N/A, not available; CEA, carcinoembryonic antigen; NPs, nanoparticles; QDs, quantum dots; IL-6, interleukin 6; SWNTS, single-walled carbon nanotubes; IL-8, interleukin 8; AuNPs, gold nanoparticles; aPR3, anti–proteinase 3; VEGF, vascular endothelial growth factor; EV71, enterovirus 71; HTS, human throat swab.

Table S2 Extinction coefficients for gold nanoparticles with various sizes (the data was obtained from TED PELLA, INC. http://www.tedpella.com/gold_html/gold-tec.htm).

Size (nm)	5	10	15	20	30	40	50	60	80	100
Extinction coefficient ($M^{-1}cm^{-1}$)	9.696×10^{6}	9.550×10^{7}	3.640×10^{8}	9.406×10^{8}	3.585×10^{9}	9.264×10^{9}	1.935×10^{10}	3.531×10^{10}	9.124×10^{10}	1.905×10^{11}

REFERENCES

1) Rissin, D. M.; Kan, C. W.; Campbell, T. G.; Howes, S. C.; Fournier, D. R.; Song, L.; Piech, T.; Patel, P. P.; Chang, L.; Rivnak, A. J.; Ferrell, E. P.; Randall, J. D.; Provuncher, G. K.; Walt, D. R.; Duffy, D. C. *Nat. Biotechnol.* **2010**, *28*, 595–599.

2) Tabakman, S. M.; Lau, L.; Robinson, J. T.; Price, J.; Sherlock, S. P.; Wang, H.; Zhang, B.; Chen, Z.; Tangsombatvisit, S.; Jarrell, J. A.; Utz, P. J.; Dai, H. *Nat. Commun.* **2011**, *2*, 466.

3) Park, J. S.; Cho, M. K.; Lee, E. J.; Ahn, K. Y.; Lee, K. E.; Jung, J. H.; Cho, Y.; Han, S. S.; Kim, Y. K.; Lee, J. *Nat. Nanotechnol.* **2009**, *4*, 259–264.

4) Hu, M.; Yan, J.; He, Y.; Lu, H.; Weng, L.; Song, S.; Fan, C.; Wang, L. *ACS Nano* **2010**, *4*, 488–494.

5) Malhotra, R.; Patel, V.; Vaqué, J. P.; Gutkind, J. S.; Rusling, J. F. *Anal. Chem.* **2010**, *82*, 3118–3123.

6) Munge, B. S.; Coffey, A. L.; Doucette, J. M.; Somba, B. K. ; Malhotra, R.; Patel, V.; Gutkind, J. S.; Rusling, J. F. *Angew. Chem., Int. Ed.* **2011**, *50*, 7915–7918.

7) Xiang, Y.; Xie, M.; Bash, R.; Chen, J. J. L.; Wang, J. *Angew. Chem., Int. Ed.* **2007**, *46*, 9054–9056.

8) Tang, D.; Yuan, R.; Chai, Y. *Anal. Chem.* **2008**, *80*, 1582–1588.

[9] Nam, J. M.; Thaxton, C. S.; Mirkin, C. A. *Science* **2003**, *301*, 1884–1886.

10) Chin, C. D.; Laksanasopin, T.; Cheung, Y. K.; Steinmiller, D.; Linder, V.; Parsa, H.; Wang, J.; Moore, H.; Rouse, R.; Umviligihozo, G.; Karita, E.; Mwambarangwe, L.; Braunstein, S. L.; van de Wijgert, J. ; Sahabo, R.; Justman, J. E.; El–Sadr, W.; Sia, S. K. *Nat. Med.* **2011**, *17*, 1015–1019.

11) Krishnan, S.; Mani, V.; Wasalathanthri, D. P.; Kumar, C. V.; Rusling, J. F. *Angew. Chem., Int. Ed.* **2011**, *50*, 1175–1178.

12) Liu, X.; Dai, Q.; Austin, L.; Coutts, J.; Knowles, G.; Zou, J.; Chen, H.; Huo. Q. *J. Am. Chem. Soc.*, **2008**, *130*, 2780–2782.

13) Chen, Z.; Tabakman, S. M.; Goodwin, A. P.; Kattah, M. G.; Daranciang, D.; Wang, X.; Zhang, G.; Li, X.; Liu, Z.; Utz, P. J.; Jiang, K.; Fan, S.; Dai, H. *Nat. Biotechnol.* **2008**, *26*, 1285–1292.

14) Li, M.; Cushing, S. K.; Zhang, J.; Suri, S.; Evans, R.; Petros, W. P.; Gibson, L. F.; Ma, D.; Liu, Y.; Wu, N. Q. *ACS Nano* **2013**, *7*, 4967–4976.

15) Rodríguez-Lorenzo, L.; de la Rica, R.; Alvarez-Puebla, R. A.; Liz-Marzán, L. M.; Stevens, M. M. *Nat. Mater.* **2012,** *11*, 604–607.

16) Inci, F.; Tokel, O.; Wang, S.; Gurkan, U. A.; Tasoglu, S.; Kuritzkes, D. R.; Demirci, U. *ACS Nano* **2013**, *7*, 4733–4745.

17) De la Rica, R.; Stevens, M. M. *Nat. Nanotechnol.* **2012**, *7*, 821–824.

18) Gao, Z.; Xu, M.; Hou, L.; Chen, G.; Tang, D. *Anal. Chem.* **2013**, *85*, 6945−6952.

19) Liu, D.; Wang, Z.; Jin, A.; Huang, X.; Sun, X.; Wang, F.; Yan, Q.; Ge, S.; Xia, N.; Niu, G.; Liu, G.; Hight Walker, A. R.; Chen, X. *Angew. Chem., Int. Ed.* **2013**, *52,* 14065–14069.